Physics in Medicine and Biology

Cone-beam CT reconstruction with gravity-induced motion

To cite this article before publication: Chun-Chien Shieh *et al* 2018 *Phys. Med. Biol.* in press https://doi.org/10.1088/1361-6560/aae1bb

Cone-beam CT Reconstruction with Gravity-induced Motion

Chun-Chien Shieh[1], Jeffrey Barber[2], William Counter[1], Jonathan Sykes[2], Peter Bennett[3], Soo-Min Heng[4], Paul White[4], Stéphanie Corde[4], Michael Jackson[4], Verity Ahern[2], Ilana Feain[5], Ricky O'Brien[1], and Paul J Keall[1]

[1]ACRF Image X Institute, The University of Sydney, NSW 2006, Australia.
[2]Western Sydney Local Health District, Blacktown, NSW 2148, Australia.
[3]Faculty of Science, The University of Sydney, NSW 2006, Australia.
[4]Nelune Comprehensive Cancer Centre, Randwick, NSW 2031, Australia.
[5]Leo Cancer Care, Redfern, NSW 2008, Australia.

E-mail: andy.shieh@sydney.edu.au

Abstract. Fixed-gantry cone-beam computed tomography (CBCT), where the imaging hardware is fixed while the subject is continuously rotated 360° in the horizontal position, has implications for building compact and affordable fixed-gantry linear accelerators (linacs). Fixed-gantry imaging with a rotating subject presents a challenging image reconstruction problem where the gravity-induced motion is coupled to the subjects rotation angle. This study is the first to investigate the feasibility of fixed-gantry CBCT using imaging data of three live rabbits in an ethics-approved study. A novel data-driven motion correction method that combines partial-view reconstruction and motion compensation was developed to overcome this challenge. Fixed-gantry CBCT scans of three live rabbits were acquired on a standard radiotherapy system with the imaging beam fixed and the rabbits continuously rotated using an in-house programmable rotation cradle. The reconstructed images of the thoracic region were validated against conventional CBCT scans acquired at different cradle rotation angles. Results showed that gravity-induced motion caused severe motion blur in all of the cases if unaccounted for. The proposed motion correction method yielded clinically usable image quality with <1 mm gravity-induced motion blur for rabbits that were securely immobilized on the rotation cradle. Shapes of the anatomic structures were correctly reconstructed with <0.5 mm accuracy. Translational motion accounted for the majority of gravity-induced motion. The motion-corrected reconstruction represented the time-averaged location of the thoracic region over a 360° rotation. The feasibility of fixed-gantry CBCT has been demonstrated. Future work involves the validation of imaging accuracy for human subjects, which will be useful for emerging compact fixed-gantry radiotherapy systems.

1. Introduction

Cone-beam computed tomography (CBCT) plays a critical role in radiotherapy as it enables subject position verification immediately before treatment. Conventionally, CBCT is acquired with the x-ray source and detector rotating around the subject. Recently, fixed-gantry radiotherapy, where the treatment beam and imaging device remain static while the subject is slowly and continuously rotated in the supine position, has been proposed (Eslick and Keall, 2015). The benefit of a fixed-gantry radiotherapy system is the massive reduction in cost and mechanical complexity needed to rotate the heavy and sophisticated linear accelerator (linac) gantry. The reduced capital and machine maintenance costs will in turn make radiotherapy much more affordable to the low- and middle-income countries that have no or minimal access to radiotherapy (Atun *et al*, 2015). Unlike conventional CBCT, fixed-gantry CBCT is acquired with the subject rotating in the horizontal position and the x-ray system fixed (Figure 1). Compared to vertical rotation (horizontal beam), horizontal rotation (vertical beam) greatly reduces the shielding requirement, and does not require a vertical CT scan. The equivalence in imaging geometry between conventional and fixed-gantry CBCT has previously been demonstrated (Feain *et al*, 2016). However, the main challenge that anatomic structures move due to gravity as the subject is horizontally rotated is yet to be addressed.

Fixed-gantry CBCT creates a new challenge in tomographic reconstruction where the motion is coupled with the acquisition angle. Uncorrected gravity-induced motion can lead to severe motion blur in the reconstruction. One way to uncouple the motion from projections is to sort projections within certain subject rotation angular ranges into "bins" and reconstructing separately, assuming that the anatomic displacements within each bin are similar. This is similar to respiratory sorting in respiratory-correlated CBCT (Sonke *et al*, 2005), except in fixed-gantry CBCT each bin would contain a narrow angular range of projections, leading to a reconstruction with limited depth information. To achieve image quality similar to that of conventional CBCT, it is necessary to utilize all the projections for the reconstruction of each bin while applying some motion correction to each projection (Rit *et al*, 2009) or each reconstructed bin (Brehm *et al*, 2012). This type of techniques, usually referred to as "motion compensation", requires prior knowledge of the motion from either the pre-treatment CT or preliminary filtered-backprojection reconstruction of the motion-resolved CBCT. Unfortunately, prior knowledge of gravity-induced motion is not viable as it is unrealistic to acquire pre-treatment CT at multiple patient rotation angles. Motion estimation from preliminary filtered-backprojection reconstruction is also difficult due to the lack of depth information.

There are several motion correction methods for tomographic imaging that do not require prior knowledge of the motion. Perrenot *et al* (2007) proposed a motion compensation technique for coronary stent reconstruction by observing the motion of the high-contrast guide wire inserted into the artery. The adoption of a similar strategy

for thoracic CBCT would require the insertion of high-contrast objects (e.g. fiducial markers), which is clinically undesirable. Berger *et al* (2016) proposed a method to estimate motion correction in weight-bearing CBCT of the knee joint, which relies on the 2D/3D registration of the bony anatomy (i.e. femur and tibia) segmented from the prior CT. The reliance on a prior CT means potential degradation in reconstruction accuracy due to changes in patient anatomy. Insertion-free data-driven approaches also exist. Wang and Gu (2016) proposed a method to simultaneously and iteratively estimate the motion and the reconstructed image, which has produced promising results for respiratory-correlated CBCT. However, this method relies on a preliminary total-variation minimization reconstruction to initialize the motion estimation. Due to the lack of depth information in each bin of a fixed-gantry CBCT reconstruction, total-variation minimization cannot yield sufficient image quality for motion estimation. Several data-driven methods (Sun *et al*, 2016; Berger *et al*, 2017; Sisniega *et al*, 2017) have been shown effective for motion correction of the head or extremities. While these methods can potentially be used to account for the rigid component of gravity-induced motion in fixed-gantry CBCT, their applicability to thoracic-abdominal imaging requires further investigation. Compared to the head and extremities, the thoracic-abdominal region contains much more soft tissue, which is more challenging to register to than large and distinct bony structure.

This study is the first to investigate the feasibility of fixed-gantry CBCT reconstruction under horizontal subject rotation. Thoracic-abdominal CBCT scans of three live rabbits under rotation were acquired in an ethics-approved study to represent fixed-gantry CBCT scans with realistic gravity-induced motion. A novel data-driven method that combines iterative reconstruction (Chen *et al*, 2008) and projection-domain motion compensation (Rit *et al*, 2009) was developed to correct for gravity-induced motion artifacts.

The rest of the paper is organized as follows. Section 2 details the acquisition of the live animal data, the workflow of the proposed reconstruction method, and also metrics used to validate the reconstructed images. Section 3 describes the validation results. Section 4 discusses the clinical implications and limitations of this study.

2. Methods

2.1. Live rabbit data

In an institution ethics committee approved study (University of Sydney Animal Ethics Project 2015/903), kilovoltage (kV) CBCT projections of three live rabbits (weighting 351, 359, and 406 g; caudal-cranial lengths approximately 22 cm) under anesthesia were acquired on the on-board imager of a Varian Truebeam (Varian Medical Systems, Palo Alto, USA). The imaging beam setting was 100 kVp, 15 mA, and 20 ms. The source-to-isocenter-distance (SID) was 1000 mm, and the source-to-detector-distance (SDD) was 1500 mm. The field-of-view (FOV) covered the thoracic and abdominal regions. The

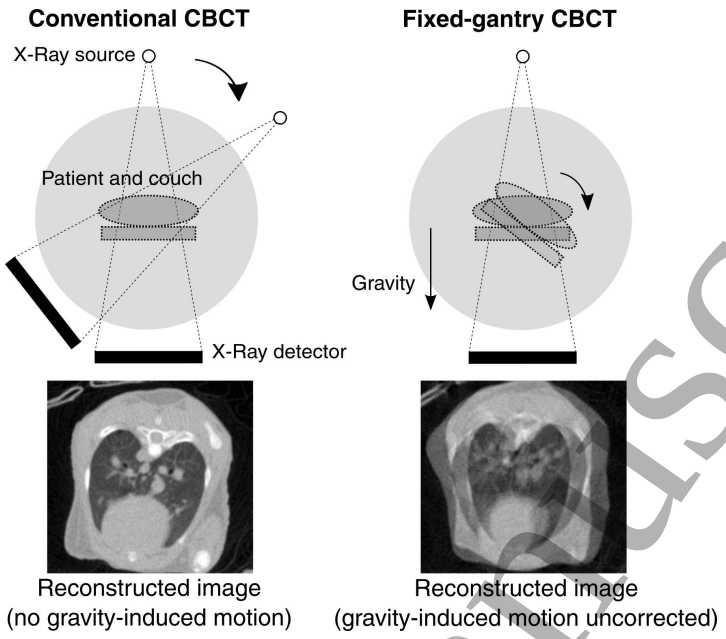

Figure 1. Conventional CBCT and fixed-gantry CBCT. Uncorrected gravity-induced motion in fixed-gantry CBCT can cause severe motion blur in the reconstruction.

rabbits were immobilized with bubble wraps and towels in a polyvinyl chloride (PVC) cradle (Figure 2) that can be rotated 360° via computer control. The rabbits were placed in a prone position, i.e. abdomen facing the bottom of the cradle. The rabbits were anesthetized during image acquisition, and were euthanized afterwards due to the amount of imaging dose they received. The rotation center of the cradle was aligned to the linac isocenter within 0.5 mm uncertainty.

Figure 3 outlines the design of this study. Both conventional CBCT (static cradle) and fixed-gantry CBCT (rotating cradle) scans were acquired for each rabbit. Conventional CBCT scans (full-fan) were acquired for each rabbit with the cradle rotated to and fixed at 0°, 45°, 90°, ..., and 315°. This process was repeated, resulting in 16 conventional CBCT scans for each rabbit. The gantry rotation speed, angular range, and imaging frequency were 6°/s, 200°, and 15 Hz. The conventional CBCT scans were reconstructed using the Feldkamp-Davis-Kress (FDK) algorithm (Feldkamp *et al*, 1984) as implemented in the Reconstruction Toolkit (Rit *et al*, 2014) with a voxel size of 0.25 mm in all three dimensions and a Hann smoothing parameter of 0.7. The conventional CBCT images provided a reference for how the anatomic structures move and deform at different rotation angles. Comparing the fixed-gantry CBCT reconstructions to the conventional CBCT reconstructions at the corresponding cradle rotation angle allowed us to estimate the spatial accuracy of fixed-gantry CBCT reconstruction. The repeated conventional CBCT scans at the same cradle rotation angles allowed us to estimate the reproducibility of motion under rotation, i.e. how similar the anatomic locations are between two full rotations at the same cradle rotation angle. More details are described in Section 2.3.

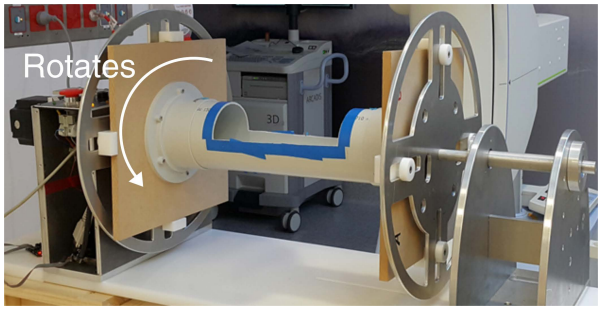

Figure 2. The rotation cradle used to hold and rotate the rabbits.

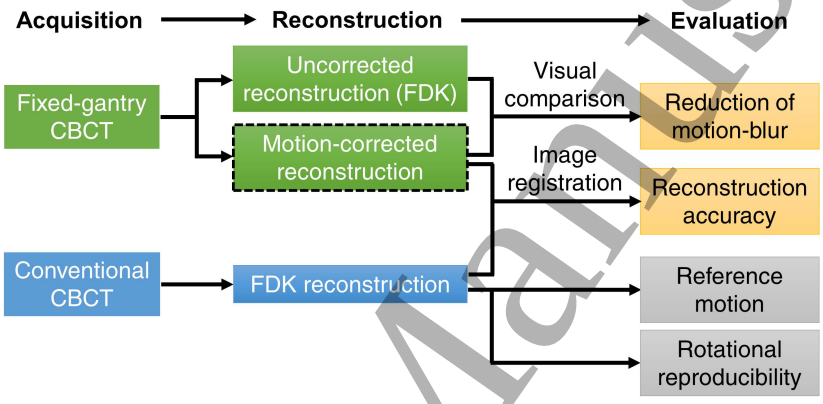

Figure 3. The flowchart of this study.

After the acquisition of the 16 conventional CBCT scans, a fixed-gantry CBCT scan was acquired for each rabbit with the x-ray source fixed at 0° and the cradle rotating at 3°/s for 360°. The imaging frequency was 15 Hz, resulting in a total of 1800 projections for each scan. The cradle rotation angle at each projection was recorded and used as the projection angle for reconstruction. The projections were then used to reconstruct an uncorrected image using the conventional FDK algorithm, and also motion-corrected images of different cradle rotation angles using our proposed method described in 2.2. The reconstruction voxel size was 0.25 mm in all three dimensions. The clinical efficacy of the motion-corrected reconstruction was evaluated in terms of motion blur and spatial match with the reference conventional CBCT reconstruction of the same cradle rotation (see 2.3 for more details). In this work, motion correction refers to the correction of gravity-induced motion blur unless otherwise specified.

2.2. CBCT reconstruction under gravity-induced motion

Our reconstruction method corrects for gravity-induced motion by combining the prior image constrained compressed sensing (PICCS) algorithm (Chen *et al*, 2008) and the motion-compensated algorithm (Rit *et al*, 2009) in a unique way. Below we give a general introduction to the PICCS and motion-compensated algorithms. The workflow of our reconstruction method is then given in Section 2.2.3.

2.2.1. Prior image constrained compressed sensing (PICCS) The PICCS algorithm (Chen *et al*, 2008) is a compressed sensing technique to mitigate undersampling artifacts in the reconstruction by imposing a similarity constraint with a prior image. In respiratory-correlated CBCT, PICCS can be used to reduce noise and streaking artifacts by using the motion-blurred 3D CBCT as the prior image. In this study, we used PICCS to compensate for the loss in depth information due to narrow angular binning. Given an undersampled projection set p and a user-specified prior image f_{Prior}, the reconstruction image $\hat{f}$ is computed by solving the following optimization problem:

$$\hat{f} = \arg\min_{f} \frac{1}{2} \|Rf - p\|^2 + \lambda \left[(1-\alpha)\, \text{TV}\,(f) + \alpha\, \text{TV}\,(f - f_{\text{Prior}}) \right], \qquad (1)$$

where R is the Radon transform, $\text{TV}\,(f)$ is the total variation of f, λ controls the strength of the regularization terms, and α controls the weighting of the prior image constraint. In this study, we used $\lambda = 1$ and $\alpha = 0.5$.

2.2.2. Motion-compensated reconstruction The motion-compensated algorithm (Rit *et al*, 2009) is a technique to correct for motion artifacts by deforming the backprojected trace in conventional FDK reconstruction using prior motion vector fields. In respiratory-correlated CBCT, the motion vector fields are calculated from the pre-treatment respiratory-correlated CT. Each backprojected trace is then deformed using a weighted sum of the two motion vector fields that best match with its respiratory phase. In this study, the motion vector fields were calculated from the PICCS reconstructions of the angularly binned projections. Instead of respiratory motion, the motion vector fields described the gravity-induced motion between different rotation angles. The backprojected trace was then deformed based on the rotation angle at which each projection was acquired.

2.2.3. Our reconstruction workflow Gravity-induced motion can be categorized into a rigid component, i.e. overall subject shift and rotation, and a deformable component. Correcting for the deformable component, which has many more parameters to be solved for than the rigid component, is often difficult in thoracic CBCT due to the lack of soft tissue contrast in projection images. Fortunately, we have found in a separate study that rigid motion accounts for 80% of gravity-induced motion in immobilized subjects (Barber *et al*, 2018). This finding suggests that correcting for the rigid component will account for most of the gravity-induced motion.

Figure 4 summarizes the proposed reconstruction method to correct for gravity-induced rigid motion, which consists of five steps. The aim of the first two steps was to preliminarily estimate motion fields describing how the subject rigidly moves (translation and rotation) as it was rotated. Firstly, the projections were sorted in terms of rotation angle into eight bins centered at 0°, 45°, ..., and 315°, each spanning a 90° angular range. Note that there was overlapping between bins, and hence each projection belonged to two bins. Reconstructions using these partial-view projections were performed using the PICCS algorithm (Chen *et al*, 2008) with the uncorrected FDK

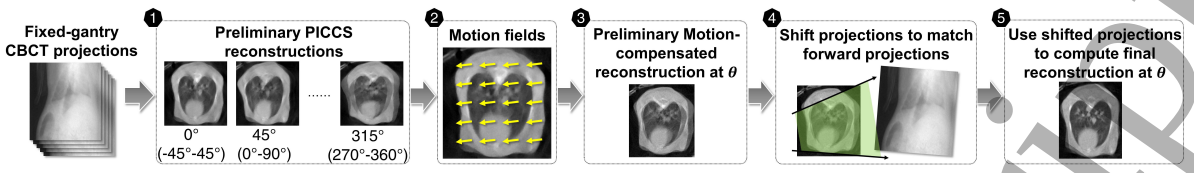

Figure 4. The workflow of the proposed reconstruction method to correct for gravity-induced motion.

reconstruction as the prior. Unlike a digital tomosynthesis reconstruction, which lacks depth information along a particular axis, PICCS can recover the depth information partially from the prior image, making it possible to estimate the gravity-induced motions at different rotation angles by 3D image registration. Secondly, the 45°, 90°, ..., and 315° reconstructions were rigidly registered to the 0° reconstruction to yield motion fields describing how the subject moved at different rotation angles.

The third step was to reconstruct the subject at a user selected rotation angle θ using the motion-compensated algorithm (Rit *et al*, 2009). The entire projection set (0°–360°) was filtered-backprojected to yield a true 3D reconstruction that does not suffer from limited depth information. To correct for gravity-induced motion, each backprojection was deformed in the 3D image space based on its rotation angle and the motion fields obtained in step two. Motion fields at rotation angles other than multiples of 45° were interpolated.

While the locations of the anatomic structures were roughly recovered from the motion compensated reconstruction, noticeable gravity-induced motion blur (around 1–5 mm) was still present at this stage. This was because the motion fields obtained in step three were extracted from preliminary reconstructions and were not completely accurate (1–4 mm mean absolute error when registered to the final reconstructions). The interpolation of motion fields was also a contributing factor. To correct for the remaining gravity-induced motion blur, the motion compensated reconstruction was forward projected to all the rotation angles during acquisition. Each of the acquired projections was then rigidly aligned to match the forward projections within a region of interest (ROI). In this study the ROI was a mask encompassing the lungs. The shifted projections represented what would have been acquired during a conventional CBCT scan with the subject rotated to and fixed at θ. The final reconstruction was then computed by FDK using the shifted projections.

2.3. Evaluation

Motion-corrected reconstructions of the rabbits at 0°, 45°, ..., and 315° cradle rotation angles were computed using the method described in the previous section. The clinical efficacy of the motion-corrected reconstruction was evaluated in terms of motion blur and spatial accuracy.

To assess motion blur, the largest blur across all axial slices of the motion-corrected reconstruction was measured visually (in mm) and compared with that measured from

the uncorrected reconstruction. Smaller motion blur indicates a sharper image.

A reconstructed image can be sharp yet spatially inaccurate such that the reconstructed anatomic structures are not in their true locations. To evaluate spatial accuracy, the fixed-gantry CBCT reconstruction was compared to the conventional CBCT image of the same cradle rotation angle, the latter considered the reference image for the true anatomic locations at that cradle rotation angle. Each motion-corrected reconstruction was first rigidly then deformably registered to the reference image within a ROI encompassing the lungs. The magnitudes of different components of the registration difference are referred to as the translational, rotational (on top of cradle rotation), and deformable reconstruction error. The rigid and B-Spline deformable registration algorithms in the *elastix* toolkit were used (Klein *et al*, 2010).

It should be noted that the conventional CBCT image was considered a reference but not a ground truth, as anatomic locations may change from rotation to rotation even at the same cradle rotation angle. To understand the uncertainty of the evaluation of spatial accuracy, it was necessary to estimate the reproducibility of gravity-induced motion under rotation. The reproducibility of motion was estimated by registering the earlier 8 conventional CBCT images (0°–315° during the first 360° rotation) to the latter 8 conventional CBCT images (0°–315° during the second 360° rotation) and computing their translational, rotational, and deformable differences. From here on, these estimates are referred to as the translational, rotational, and deformable uncertainties.

To provide perspectives for the scale of errors and uncertainties, the gravity-induced motions observed from the conventional CBCT images at different cradle rotation angles (relative to 0° rotation) were also computed. These observed gravity-induced motions are referred to as the translational, rotational, and deformable reference motions.

3. Results

Figure 5 compares the uncorrected reconstructions of fixed-gantry CBCT to the motion-corrected reconstructions and the conventional CBCT images of 0° cradle rotation. The findings from the reconstructions at 0° cradle rotation were representative of other cradle rotation angles. The motion-uncorrected reconstructions exhibited severe motion blur in the form of the "doubling" artifacts of anatomic structures. Gravity-induced motion blur was significantly reduced in the motion-corrected reconstructions. Qualitatively, the motion-corrected reconstructions of rabbit 1 and 2 exhibited sufficient clarity to identify structures such as the rib cage, spine, lung boundary, and some of the fine pulmonary structures. High similarity between the motion-corrected reconstructions and the conventional CBCT images was also evident. For rabbit 3, the motion-corrected reconstruction still exhibited noticeable motion blur despite considerable improvement compared to the uncorrected reconstruction. The motion-corrected reconstruction was also dissimilar to the conventional CBCT image. The inferior reconstruction outcomes were likely because rabbit 3 underwent much larger gravity-induced motion during rotation as later shown in Table 1. Figure 6 compares the motion-corrected fixed-

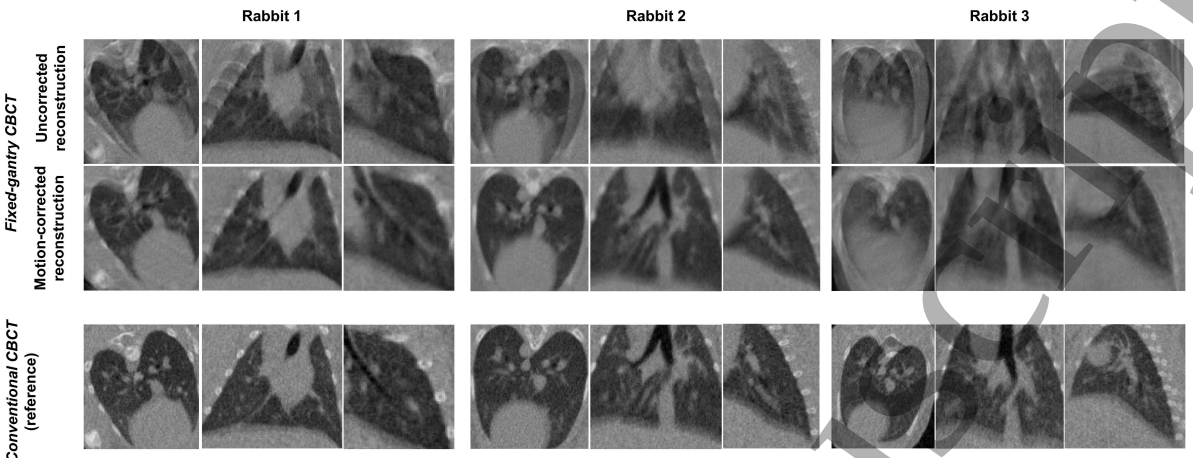

Figure 5. The uncorrected and motion-corrected (0° cradle rotation) reconstruction of fixed-gantry CBCT compared with conventional CBCT (0° cradle rotation) in axial, coronal, and sagittal view. Windowing level: [0, 0.03] mm^{-1}.

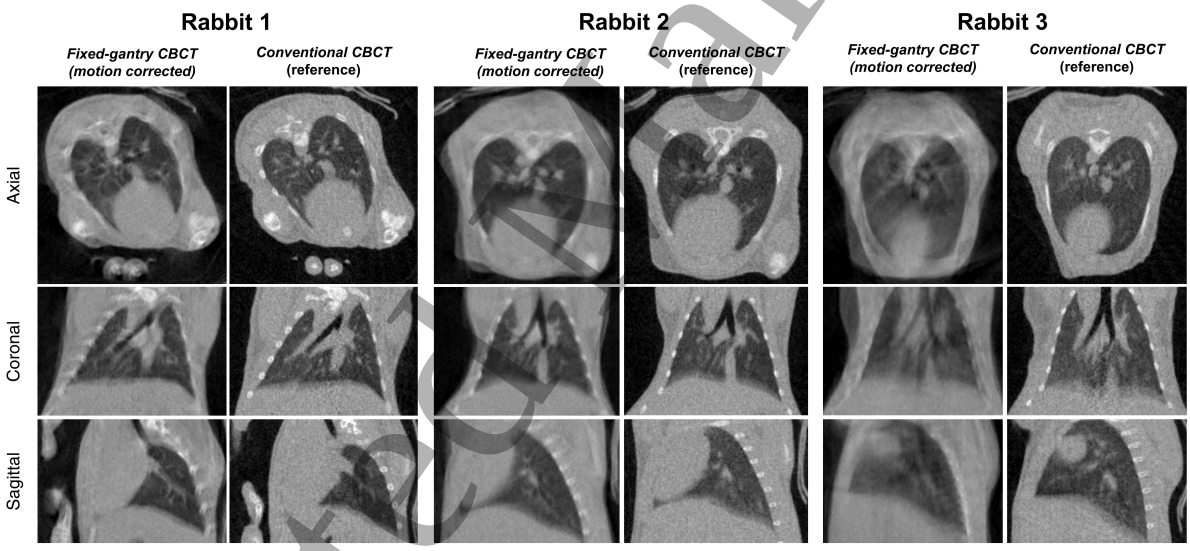

Figure 6. The motion-corrected (135° cradle rotation) reconstruction of fixed-gantry CBCT compared with conventional CBCT (135° cradle rotation) in axial, coronal, and sagittal view. All the images have been rotated to 0° cradle rotation for display purpose. Windowing level: [0, 0.03] mm^{-1}.

gantry CBCT to the conventional CBCT images at 135° cradle rotation. Similar to the observations from Figure 5, motion blur was significantly reduced in the motion-corrected reconstructions, which rendered sufficient clarity for structures inside and around the lungs for rabbit 1 and 2. The skin and extremities of the subjects suffered from more residual blur than the lungs. This is because the proposed method was implemented to correct for motion within a ROI encompassing the lungs (cf. Section 2.2.3).

Figure 7 compares the maximum motion blur observed from the uncorrected and motion-corrected reconstructions of fixed-gantry CBCT. Motion blur was evaluated by

Table 1. The mean (maximum) magnitudes across different cradle rotation angles of the translation, pitch, yaw, roll, and mean deformation magnitude of the reconstructed geometric errors, uncertainties, and reference motion.

Rabbit	Component	Reconstruction error	Uncertainty	Reference motion
1	Translation (mm)	3.3 (4.9)	1.1 (2.1)	4.4 (6.6)
	Pitch (°)	1.0 (1.8)	0.3 (1.0)	1.3 (2.4)
	Yaw (°)	0.8 (1.3)	0.2 (0.4)	1.1 (2.2)
	Roll (°)	2.1 (4.3)	3.1 (3.9)	3.2 (5.7)
	Mean deformation (mm)	0.4 (0.5)	0.2 (0.3)	0.3 (0.4)
2	Translation (mm)	3.8 (4.4)	1.1 (1.6)	4.6 (7.5)
	Pitch (°)	0.7 (1.5)	0.6 (1.1)	0.9 (1.4)
	Yaw (°)	0.6 (0.9)	0.8 (1.5)	0.4 (1.3)
	Roll (°)	2.7 (4.3)	2.1 (3.8)	1.8 (3.4)
	Mean deformation (mm)	0.3 (0.5)	0.2 (0.4)	0.5 (0.6)
3	Translation (mm)	6.7 (9.7)	4.0 (5.1)	7.5 (10.4)
	Pitch (°)	2.0 (3.4)	1.8 (4.0)	3.0 (4.8)
	Yaw (°)	0.9 (1.8)	0.4 (0.7)	0.6 (0.9)
	Roll (°)	6.0 (11.5)	3.6 (6.2)	7.2 (10.6)
	Mean deformation (mm)	0.6 (0.9)	0.4 (0.5)	0.9 (1.2)

measuring the extent of the doubling artifacts, which can be clearly seen around the boundaries of the lungs. The largest motion blur was observed in the axial plane and generally approximately in the left-right direction. As respiratory motion generally has minimal impact in the left-right direction, we expect the measured blur to be mainly caused by gravity. The motion-corrected reconstructions resulted in significantly smaller motion blur compared to the uncorrected reconstructions regardless of the cradle rotation angle. The observed motion blur was <0.75 mm, <0.5 mm, and <3.0 mm for rabbit 1, 2, and 3. The mean reduction in motion blur was 4.7 mm, 3.7 mm, and 8.2 mm for each of the rabbits.

Figure 8 shows the difference images between the motion-corrected fixed-gantry CBCT reconstructions and the corresponding reference images after rigid alignment. The differences represent the effects of geometric error due to anatomic deformation as well as residual motion blur in the motion-corrected reconstructions. For rabbit 1 and 2, differences within the lungs appeared to be minimal, but slight residual motion blur around the anterior boundaries of the lungs can be seen. For rabbit 3, image difference due to anatomic deformation and residual motion blur can still be clearly observed.

To gain a more detailed insight into the spatial accuracy of fixed-gantry CBCT reconstruction and magnitude of gravity-induced motion under rotation, Table 1 summarizes the mean and maximum magnitudes (across different cradle rotation angles) of the reconstruction errors, uncertainties, and reference motion in terms of

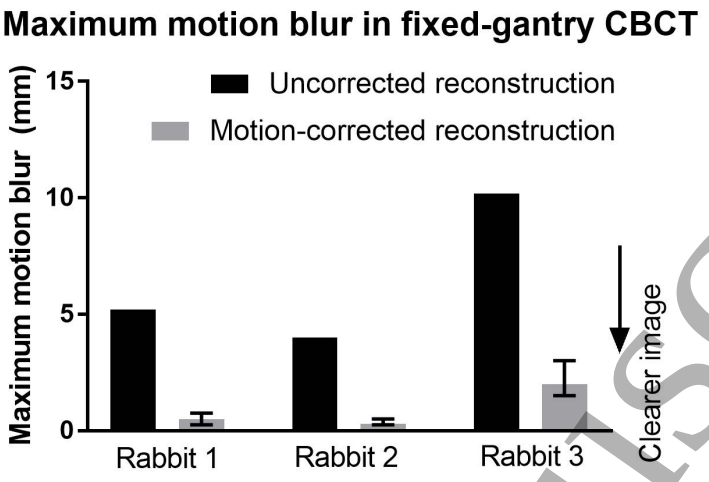

Figure 7. The maximum motion blur observed from the uncorrected and motion-corrected reconstructions of fixed-gantry CBCT scans. For the motion-corrected reconstructions, the maximum motion blur averaged across different cradle rotation angles were plotted, with the error bars representing the standard deviations.

the translational, rotational, and deformable components.

Based on different components of the reference motion, it is clear that translation accounted for the majority of gravity-induced motion. Overall the translational reconstruction error was smaller than the translational reference motion, meaning that fixed-gantry CBCT does improve subject positioning accuracy. For rabbit 1 and 2, the maximum translational reconstruction error was <5 mm. However, the translational reconstruction error was higher than the translational uncertainty. This indicates that the reconstruction errors were not simply attributed to the reproducibility of gravity-induced motion, but also because fixed-gantry CBCT reconstruction failed to accurately represent the actual translational motion that occurred during rotation.

It was difficult to conclude the rotational and deformable components of the geometric error as the corresponding uncertainties were of very similar magnitudes. However, gravity-induced rotation and deformation were very small compared to translation and appeared to be a minor concern for fixed-gantry radiotherapy. For rabbit 1 and 2, the largest reference rotation and deformation was only 5.7° (roll) and 0.6 mm.

Table 1 confirms that rabbit 3 experienced much larger gravity-induced motion than the other two rabbits, which was likely because rabbit 3 was much more loosely immobilized on the rotation cradle. The much larger gravity-induced motion caused the larger residual motion blur and larger reconstruction error. This result suggests that proper immobilization is crucial for fixed-gantry CBCT reconstruction.

To further understand the cause of the translational reconstruction error, Figure 9 shows the reconstructed and reference translational motion of the thoracic region in the left-right (LR), superior-inferior (SI), and anterior-posterior (AP) directions. The 0° conventional CBCT was used as the reference point of zero translation. It can be

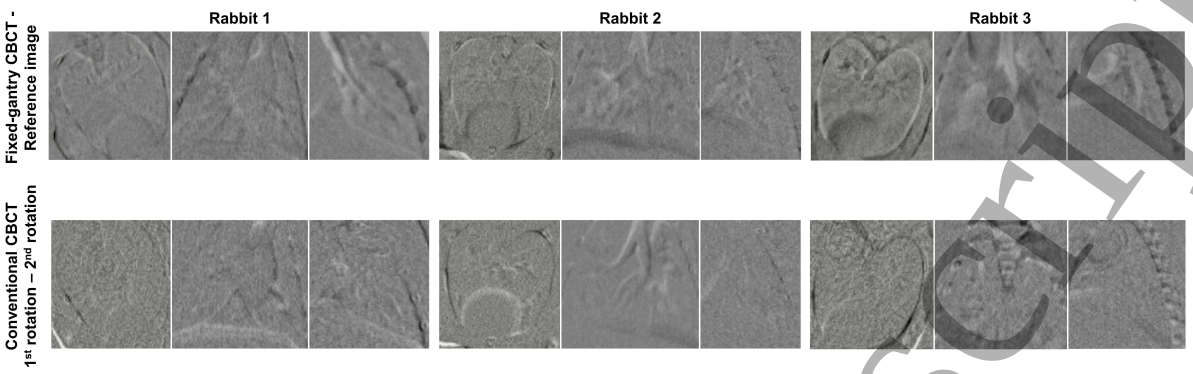

Figure 8. (Upper row) Difference images between the motion-corrected fixed-gantry CBCT reconstructions (0° cradle rotation) and the corresponding reference images, i.e. conventional CBCT images of 0° cradle rotation. (Lower row) Difference images between the conventional CBCT images of 0° cradle rotation acquired during the first and second repetitions of 360° rotation, which represent the uncertainty in measuring spatial accuracy due to the reproducibility of anatomic motion between different rotations. In both cases, the difference images were calculated after rigidly aligning the images. The differences thus represent the effects of geometric error due to anatomic deformation as well as residual motion blur in the motion-corrected reconstructions. Windowing level: [-0.02, 0.02] mm^{-1}.

seen that in general the reference LR and AP translations followed a sine and cosine patterns with respect to the cradle rotation angle as one would expect. Reference SI translation generally remained at zero except for rabbit 3, which was likely due to loose immobilization. The reconstructed LR and AP translations did not match the reference translations. For rabbit 1 and 2, they roughly remained at the average locations of the reference translations. In other words, the fixed-gantry CBCT reconstructions "saw" the subject remain roughly static around the mean position during a 360° rotation. This result will be further discussed in Section IV. The reconstructed SI translation agreed closely with the reference SI translation for rabbit 1. For rabbit 2, there was an offset of 2 mm, which is likely due to sliding motion that occurred between the conventional CBCT scans and the fixed-gantry CBCT scan. For rabbit 3, the reconstructed translations were likely unreliable due to the inferior image quality caused by improper immobilization, which may have affected the accuracy of image registration.

4. Discussion

We have investigated the feasibility of fixed-gantry CBCT reconstruction under gravity-induced motion, which have implications for building compact and affordable fixed-gantry linacs (Feain *et al*, 2016). A novel data-driven reconstruction method was developed, implemented, and evaluated to overcome the challenge of the coupling between projection acquisition and gravity-induced motion due to subject rotation. Evaluation of the proposed method was performed using kV imaging data of three live rabbits acquired on a standard radiotherapy system, the findings of which are

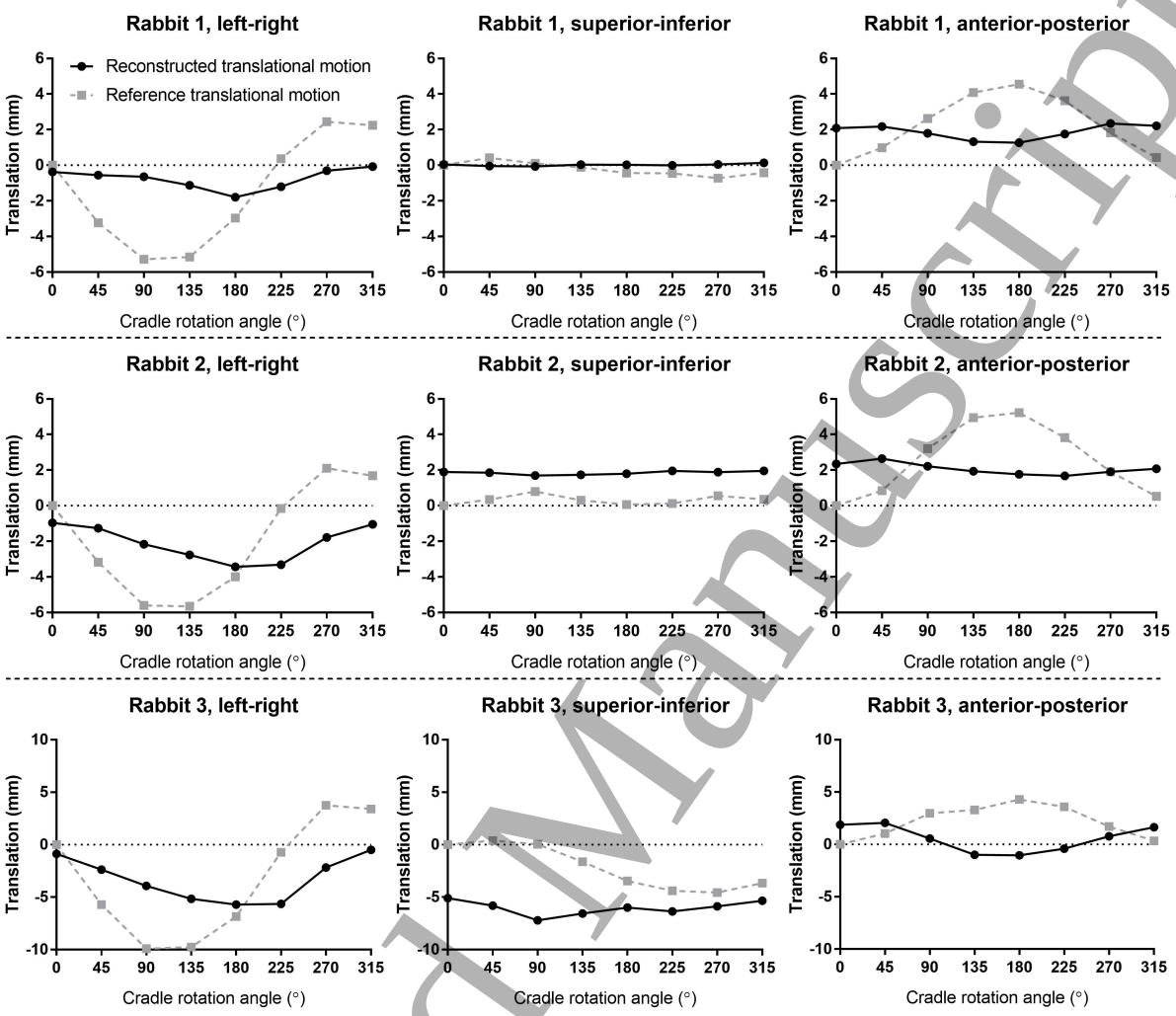

Figure 9. The translational motion in the LR, SI, and AP directions observed from the fixed-gantry CBCT reconstructions and the conventional CBCT reconstructions. The 0° conventional CBCT was used as the reference point of zero translation. LR: left-right; SI: superior-inferior; AP: anterior-posterior.

summarized below.

Gravity-induced motion was found to cause severe motion blur that hinders the clinical use of fixed-gantry CBCT if uncorrected for. The proposed motion-corrected reconstruction method was proven highly effective in reducing gravity-induced motion blur. It can produce reconstructed images with clinically usable quality (<1 mm motion blur) for lagomorph subjects that are immobilized securely such that they do not experience large and chaotic motion during rotation. We found in this study that motion-corrected reconstructions of subjects that experience <6 mm motion in each of the directions during rotation, e.g. rabbit 1 and 2, show negligible motion blur. On the other hand, motion-corrected reconstructions of subjects that experienced >10 mm motion in each of the directions, e.g. rabbit 3, can exhibit noticeable motion blur even after significant reduction compared to the motion-

uncorrected reconstruction. Larger subject motion leads to more motion blur in the preliminary partial-view reconstructions, which degrade the estimation of motion fields, and therefore compromising the outcomes of the motion compensation reconstruction. The variability in motion range observed in this study is likely due to the inconsistency in applying the immobilization strategy consisting of bubble wraps and towels. The concern of suffocating or hurting the rabbits may have caused the immobilization for rabbit 3 to be much looser than the other rabbits. The shape of the rabbit body may also have an effect. Whelan *et al* (2017) showed that a combination of pressurized air bags and straps can rotate a human subject securely and stably, with a mean average surface distance of the prostate between different rotation angles of 3.76 mm. The healthy volunteer in that study did not report any substantial discomfort during or after the rotation.

In terms of spatial accuracy, the motion-corrected reconstruction can recover the shape of the anatomic structures accurately (<0.5 mm deformable difference) for securely immobilized subjects, indicating that the proposed method does not distort the reconstructed image. Although the proposed reconstruction method does not account for deformable motion during rotation, in this cohort deformation was not found to be a concern as anatomic structures undergo minimal deformation during rotation as indicated by the results. Translational motion, on the other hand, accounts for the majority of gravity-induced motion during rotation. For securely immobilized subjects, SI translation was found to be minimal while the LR and AP translation follow sinusoidal patterns. The results indicated that while the motion-corrected reconstruction does not correctly recover the range of the motion, it represents a time-averaged position of the sinusoidal pattern over a 360° rotation.

The reason why the motion-corrected reconstruction represents the time-averaged position is that the majority of the gravity-induced motion is downward, which is along the imaging beam direction in the case of this study. This is evident from Figure 9 as the sinusoidal pattern of the observed motion was a result of the angle between the direction of gravity and the patient axes, which varied according to the cradle rotation angle. For the level of beam divergence in common radiotherapy imaging, e.g. SDD around 1500 mm and detector size around 400 mm, motion along the imaging beam direction is mostly unobservable. In other words, if the imaging source is positioned at 0° (i.e. pointing towards the ground), the fixed-gantry CBCT projections can barely resolve motion along the direction of gravity regardless of the reconstruction method. Nevertheless, if the treatment beam is also parallel to the direction of gravity, the motion unresolved on the fixed-gantry CBCT will be of minimal concern for photon therapy since the dose distribution of photon falls off slowly and is therefore forgiving to uncertainty. Consequently, for fixed-gantry photon radiotherapy, it would be wise to place both the treatment beam and the imaging beam as parallel to the direction of gravity as possible. An interesting future study would be to investigate the feasibility of fixed-gantry CBCT with the kV source placed at 90°.

Several data-driven methods (Sun *et al*, 2016; Berger *et al*, 2017; Sisniega *et al*,

2017) have been shown effective for motion correction of the head or extremities. The use of these methods to account for the rigid component of gravity-induced motion is possible, but requires further investigation. Berger *et al* (2017) used Fourier consistency conditions to apply motion corrections to a digital head and knee phantom. Its application to real clinical images is yet to be studied. Sisniega *et al* (2017) used a penalized image sharpness criterion for motion correction in extremity CBCT, which was shown to be effective on a clinical dataset of a lower extremity. The applicability of the penalized image sharpness criterion to the thoracic-abdominal region, which contains a lot more soft tissue than large and distinct bony structure, warrants further study. Sun *et al* (2016) utilized expectation maximization reconstruction to correct for rigid motion in head CT scans. Its efficacy under the additional scatter noise in CBCT projections has not yet been studied. Computation time (14 hours) is also a practical challenge. With partial graphical processing unit implementation, the computation time of our proposed method is currently around 30 minutes.

There are several limitations of the study. Firstly, the proposed reconstruction method corrects for only the rigid component of gravity-induced motion. While results have shown that this is a very promising first-order correction, future work should focus on further correcting for the deformable components. From a healthy human volunteer, Whelan *et al* (2017) found that the deformable component accounts for 0.87±0.25, 1.75±0.77, and 2.81±1.12 mm mean average surface distance of the prostate, rectum, and bladder from the non-rotated position. Secondly, the conventional CBCT images of different cradle rotation angles acquired before the fixed-gantry CBCT scans could not serve as the absolute ground truth for the motion-corrected reconstruction because even at the same cradle rotation angle, anatomic structures can still move between different repetitions of 360° rotation. Although uncertainty due to this movement was estimated based on repeated conventional CBCT scans, it could have been over- or under-estimated as two repetitions of 360° may not accurately represent the true variation in anatomic locations. Thirdly, the results obtained from rabbits may not be representative of human subjects due to the obvious difference in size and weight. As it is generally not feasible to impose high imaging radiation dose on a human subject, animal models have been used throughout the history of radiotherapy research as a pioneering strategy. To provide some perspectives, in this study the diaphragmatic motion was found to be around 2 mm for rabbit 1 and 2, and around 4.5 mm for rabbit 3, which was roughly half the magnitude of the gravity-induced motion they experienced. The length of the lungs of the rabbits in the SI direction ranged from 30–35 mm. Whether gravity-induced motion and the related reconstruction accuracy would scale with the size of the lung or the amplitude of respiratory motion warrants further investigation. Additionally, there will be more scatter noise from a human subject than from a rabbit due to the much bigger subject size, which may affect the reconstruction outcome. Fourthly, in contrast to the conventional FDK algorithm, which is exact in nature for the central axial plane, motion-compensated filtered-backprojection is likely approximate in every axial plane. This limitation can potentially be overcome by adopting an exact reconstruction technique

for dynamic fan-beam CT proposed by Roux *et al* (2004). Finally, this study has not accounted for the second largest contributing factor to motion blur in the thoracic region - respiratory motion. Future work involves the integration of the proposed method with existing techniques to correct for respiratory motion. A potential solution is to sort the gravity-induced motion-corrected projections into respiratory bins (Sonke *et al*, 2005). Another solution is motion-compensated reconstruction (Rit *et al*, 2009) using both the gravity-induced motion vector fields (calculated in this study) and respiration-induced motion vector fields (calculated from respiratory-correlated CT).

5. Conclusion

For the first time, the feasibility of fixed-gantry CBCT reconstruction under gravity-induced motion was investigated using imaging data of three live rabbits. A novel data-driven reconstruction approach was developed to overcome the challenge of the coupling between motion and acquisition angle. Without motion correction, fixed-gantry CBCT suffers from severe motion blur, which makes it clinically unusable. The proposed motion correction method can reconstruct clinically useful images for subjects that are securely immobilized on the treatment couch. With the proposed motion correction method, clinically useful image quality with <1 mm motion blur can be achieved. The shapes of the anatomic structures are also reconstructed with <0.5 mm accuracy. The motion-corrected reconstruction represents the time-averaged location of the thoracic region over a 360° rotation. These results have implications for building compact and affordable fixed-gantry linacs that can potentially provide wide access to radiotherapy for low- and middle-income countries. Future work involves the investigation of imaging accuracy for human subjects using dedicated patient rotation system (Ilana *et al*, n.d.).

Acknowledgments

We would like to thank Simon Downes at the Nelune Comprehensive Cancer Centre for assisting us with the experimental procedure, and Ms Christine Chen for providing valuable feedback. We acknowledge the funding support from the Australian Government National Health and Medical Research Council Development Grant APP1118450, Early Career Fellowship APP1120333, and Cancer Institute New South Wales Early Career Fellowship CS00481.

Conflict of interest

Author Feain is an employee and shareholder, and author Keall is a shareholder of Leo Cancer Care, a radiation therapy machine company that incorporates patient rotation. Authors Feain and Keall are inventors on several pending patents involving patient rotation during radiotherapy.

References

Atun R, Jaffray D A, Barton M B, Bray F, Baumann M, Vikram B, Hanna T P, Knaul F M, Lievens Y, Lui T Y M, Milosevic M, O'Sullivan B, Rodin D L, Rosenblatt E, Dyk J V, Yap M L, Zubizarreta E and Gospodarowicz M 2015 Expanding global access to radiotherapy *The Lancet Oncology* **16**(10), 1153 – 1186.
URL: *http://www.sciencedirect.com/science/article/pii/S1470204515002223*

Barber J, Shieh C C, Counter W, Sykes J, Bennett P, Ahern V, Corde S, Heng S M, White P, Jackson M, Liu P, Keall P J and Feain I 2018 A CBCT study of the gravity-induced movement in rotating rabbits *PHYSICS IN MEDICINE AND BIOLOGY* **63**(10).

Berger M, Mller K, Aichert A, Unberath M, Thies J, Choi J, Fahrig R and Maier A 2016 Marker-free motion correction in weight-bearing cone-beam ct of the knee joint *Medical Physics* **43**(3), 1235–1248.
URL: *https://aapm.onlinelibrary.wiley.com/doi/abs/10.1118/1.4941012*

Berger M, Xia Y, Aichinger W, Mentl K, Unberath M, Aichert A, Riess C, Hornegger J, Fahrig R and Maier A 2017 Motion compensation for cone-beam CT using Fourier consistency conditions *PHYSICS IN MEDICINE AND BIOLOGY* **62**(17), 7181–7215.

Brehm M, Paysan P, Oelhafen M, Kunz P and Kachelriess M 2012 Self-adapting cyclic registration for motion-compensated cone-beam CT in image-guided radiation therapy *Medical Physics* **39**(12), 7603–7618.

Chen G H, Tang J and Leng S 2008 Prior image constrained compressed sensing (piccs): A method to accurately reconstruct dynamic ct images from highly undersampled projection data sets *Medical physics* **35**(2), 660–663.
URL: *http://www.ncbi.nlm.nih.gov/pmc/articles/PMC2655145/*

Eslick E M and Keall P J 2015 The nano-x linear accelerator: A compact and economical cancer radiotherapy system incorporating patient rotation *Technology in Cancer Research & Treatment* **14**(5), 565–572. PMID: 24949649.
URL: *https://doi.org/10.7785/tcrt.2012.500436*

Feain I, Shieh C C, White P, O'Brien R, Fisher S, Counter W, Lazarakis P, Stewart D, Downes S, Jackson M, Baxi S, Whelan B, Makhija K, Huang C Y, Barton M and Keall P 2016 Functional imaging equivalence and proof of concept for image-guided adaptive radiotherapy with fixed gantry and rotating couch *Advances in Radiation Oncology* **1**(4), 365–372.
URL: *http://www.ncbi.nlm.nih.gov/pmc/articles/PMC5514241/*

Feldkamp L A, Davis L C and Kress J W 1984 Practical cone-beam algorithm *J. Opt. Soc. Am. A* **1**(6), 612–619.
URL: *http://josaa.osa.org/abstract.cfm?URI=josaa-1-6-612*

Ilana F, Lloyd C, Hue W, Richard S, Ricky O and Paul K n.d. Technical Note: The design and function of a horizontal patient rotation system for the purposes of fixed-

beam cancer radiotherapy *Medical Physics* **44**(6), 2490–2502.
URL: *https://aapm.onlinelibrary.wiley.com/doi/abs/10.1002/mp.12219*

Klein S, Staring M, Murphy K, Viergever M and Pluim J 2010 elastix: a toolbox for intensity-based medical image registration *IEEE Transactions on Medical Imaging* **29**(1), 196 – 205.

Perrenot B, Vaillant R, Prost R, Finet G, Douek P and Peyrin F 2007 Motion correction for coronary stent reconstruction from rotational X-ray projection sequences *IEEE TRANSACTIONS ON MEDICAL IMAGING* **26**(10), 1412–1423.

Rit S, Oliva M V, Brousmiche S, Labarbe R, Sarrut D and Sharp G C 2014 The Reconstruction Toolkit (RTK), an open-source cone-beam CT reconstruction toolkit based on the Insight Toolkit (ITK) *XVII INTERNATIONAL CONFERENCE ON THE USE OF COMPUTERS IN RADIATION THERAPY (ICCR 2013)* **489**. 17th International Conference on the Use of Computers in Radiation Therapy (ICCR), Australasian Coll Phys Scientists & Engineers Med, Melbourne, AUSTRALIA, MAY 06-09, 2013.

Rit S, Wolthaus J W H, van Herk M and Sonke J J 2009 On-the-fly motion-compensated cone-beam ct using an a priori model of the respiratory motion *Medical Physics* **36**(6Part1), 2283–2296.
URL: *http://dx.doi.org/10.1118/1.3115691*

Roux S, Desbat L, Koenig A and Grangeat P 2004 Exact reconstruction in 2D dynamic CT: compensation of time-dependent affine deformations *PHYSICS IN MEDICINE AND BIOLOGY* **49**(11), 2169–2182. 7th International Conference on Fully Three-Dimensional Reconstruction in Radiation and Nuclear Medicine, Saint Malo, FRANCE, JUN 30-JUL 04, 2003.

Sisniega A, Stayman J W, Yorkston J, Siewerdsen J H and Zbijewski W 2017 Motion compensation in extremity cone-beam CT using a penalized image sharpness criterion *PHYSICS IN MEDICINE AND BIOLOGY* **62**(9), 3712–3734.

Sonke J J, Zijp L, Remeijer P and van Herk M 2005 Respiratory correlated cone beam ct *Medical Physics* **32**(4), 1176–1186.
URL: *http://dx.doi.org/10.1118/1.1869074*

Sun T, Kim J H, Fulton R and Nuyts J 2016 An iterative projection-based motion estimation and compensation scheme for head x-ray CT *Medical Physics* **43**(10), 5705–5716.

Wang J and Gu X 2016 Simultaneous motion estimation and image reconstruction (smeir) for 4d conebeam ct *Medical Physics* **40**(10), 101912.
URL: *https://aapm.onlinelibrary.wiley.com/doi/abs/10.1118/1.4821099*

Whelan B, Liney G P, Dowling J A, Rai R, Holloway L, McGarvie L, Feain I, Barton M, Berry M, Wilkins R and Keall P 2017 An mri-compatible patient rotation system design, construction, and first organ deformation results *Medical Physics* **44**(2), 581–588.
URL: *http://dx.doi.org/10.1002/mp.12065*